

Displacement of Molecules near a Metal Surface as Seen by an SPR–SPFS Biosensor

Sanong Ekgasit,^{*,†,‡} Fang Yu,[‡] and Wolfgang Knoll[‡]

Sensor Research Unit, Department of Chemistry, Faculty of Science, Chulalongkorn University, Bangkok 10330, Thailand, and Max-Planck-Institut für Polymerforschung, Ackermannweg 10, D-55128 Mainz, Germany

Received September 7, 2004. In Final Form: February 18, 2005

Movement of a fluorophore-labeled antibody on the surface of a self-assembled monolayer (SAM) was observed by surface plasmon resonance and surface-plasmon field-enhanced fluorescence spectroscopy (SPFS). At an extremely low surface coverage, the antibody lies close to the biotin-functionalized SAM surface. As additional nonlabeled antibodies were bound, the fluorophore-labeled antibody was displaced away from the SAM surface (and thus the gold surface) due to the constraint imposed by the neighboring nonlabeled antibody. A greater SPFS fluorescence signal was observed due to the weaker fluorescence quenching at large distances from the gold surface. The magnitude of the displacement is proportional to the available biotin binding sites on the sensor surface. The displacement is theoretically explained on the basis of the relationship between the fluorescence intensity and the evanescent field amplitude within the dielectric medium.

Introduction

Surface plasmon resonance (SPR) spectroscopy has proven to be a powerful affinity biosensor and is an accepted bioanalytical technique for routine characterization of molecular recognition events at the interface. SPR spectroscopy takes advantage of the strong surface-plasmon-wave-generated evanescent field at the metal/dielectric interface for probing thin dielectric films deposited on the metal surface. The exponential decay characteristic of the evanescent field makes the SPR sensor very sensitive to physicochemical phenomena at the interface. The kinetics of the reactions, binding events, and properties of the dielectric film can be studied via the resonance angle shift and/or the reflectance change. As the refractive index and/or the thickness of the dielectric film is changed by the interaction, the resonance angle shifts to a new position. The linear relationship between the change of SPR signal and the refractive index and/or thickness variation enables SPR to quantitatively analyze the physicochemical phenomena at the interface.¹

Since an observable change in the SPR curve is induced by thickness and/or refractive index variations, binding events associated with a small number of molecules and/or small molecules cannot be detected by SPR due to insufficient refractive index and/or thickness changes associated with the binding events. By combining the strong SPR-generated evanescent field and the highly sensitive nature of fluorescence spectroscopy, such binding events can be clearly observed by surface-plasmon field-enhanced fluorescence spectroscopy (SPFS). The highly surface-sensitive SPFS is proven to be a complementary to SPR where chemical information (i.e., fluorophore-

labeled or nonfluorophore-labeled molecule) together with the physical information (i.e., thickness and refractive index of the dielectric film) can be collected simultaneously.²

Although SPFS is a very sensitive SPR-based sensing technique, quantitative analysis of the fluorescence signal is complicated by the fluorescence quenching via the nonradiative resonance energy transfer (RET) near the metal surface. The fluorescence intensity decreases substantially as the fluorophore is confined close to the metal surface.³ Although the fluorescence quenching is an undesirable phenomenon, the distance-dependent RET can be employed for the determination of the relative separation of the fluorophore-containing molecules from the metal surface under various conditions. This paper will show that a small displacement of fluorophore-labeled antibody imposed by neighboring nonlabeled antibodies can be observed by the SPR–SPFS technique. The displacement will be theoretically explained by the relationship between the fluorescence intensity and the evanescent field amplitude within the dielectric medium.

Theory

SPR Reflectance. SPR reflectance of a multilayer biosensor depends strongly on the experimental conditions (i.e., angle of incidence and wavelength of the coupled radiation) and material characteristics (i.e., complex dielectric constants of the metal film, dielectric films and the dielectric substrate, and thickness of the metal film and dielectric films). Under the ATR condition, the

(2) (a) Liebermann, T.; Knoll, W. *Colloids Surf., A* **2000**, *171*, 115–130. (b) Liebermann, T.; Knoll, W. *Langmuir* **2003**, *19*, 1567–1572. (c) Yu, F.; Yao, D. F.; Knoll, W. *Anal. Chem.* **2003**, *75*, 2610–2617. (d) Roy, S.; Kim, J.; Kellis, J. T., Jr.; Poullose, A. J.; Robertson, C. R.; Gast, A. P. *Langmuir* **2002**, *18*, 6319–6323. (e) Nagamura, T.; Yamamoto, M.; Terasawa, M.; Shiratori, K. *Appl. Phys. Lett.* **2003**, *83*, 803–805. (f) Schütt, M.; Krupka, S. S.; Milbradt, A. G.; Deindl, S.; Sinner, E.-K.; Oesterheld, D.; Renner, C.; Moroder, L. *Chem. Biol.* **2003**, *10*, 487–490.

(3) (a) Barnes, W. L. *J. Mod. Optics* **1998**, *45*, 661–699. (b) Wokaun, A.; Lutz, H. P.; King, A. P.; Wild, U. P.; Ernst, R. R. *J. Chem. Phys.* **1983**, *79*, 509–514. (c) Lakowicz, J. R. *Anal. Biochem.* **2001**, *298*, 1–24. (d) Pockrand, I.; Brillante, A.; Möbius, D. *Chem. Phys. Lett.* **1980**, *69*, 499–504. (e) Daffertshofer, M.; H. Port, H.; Wolf, H. C. *Chem. Phys.* **1995**, *200*, 225–233.

* Author to whom correspondence should be addressed. E-mail: sanong.e@chula.ac.th.

[†] Chulalongkorn University.

[‡] Max-Planck-Institut für Polymerforschung.

(1) (a) Raether, H. *Surface Plasmon on Smooth and Rough Surfaces and on Gratings*; Springer-Verlag: Berlin, Heidelberg, 1988; Vol. 111. (b) Knoll, W. *Annu. Rev. Phys. Chem.* **1998**, *49*, 569–638. (c) Homola, J.; Yee, S. S.; Gauglitz, G. *Sens. Actuators, B* **1999**, *54*, 3–15. (d) Salamon, Z.; Macleod, H. A.; Tollin, G. *Biochim. Biophys. Acta* **1997**, *1331*, 117–129. (e) Homola, J. *Anal. Bioanal. Chem.* **2003**, *377*, 528–539.

reflectance, $R(\theta)$, with a parallel-polarized radiation can be expressed in terms of the optical constants and the evanescent field amplitude by⁴

$$R(\theta) = 1 - A(\theta) = 1 - \left(\frac{2\pi}{\lambda}\right)^2 \frac{1}{k_{zP}(\theta)} \sum_{j=1}^N \int_{z_j}^{z_{j+1}} \text{Im}[\hat{\epsilon}_j] \langle E_z^2(\theta) \rangle dz \quad (1)$$

where θ is the angle of incidence, $A(\theta)$ is the absorption in the *absorbance unit*, λ is the wavelength of the coupled radiation, $\hat{\epsilon}_j$ is the complex dielectric constant of the j^{th} layer, and $\langle E_z^2(\theta) \rangle$ is the mean square evanescent electric field (MSEF) at a distance z from the prism/metal interface. N is the number of layers in the sensor architecture with the metal film as the first layer. $k_{zP}(\theta)$ is the z component of the wavevector in the prism. $k_{zP}(\theta)$ can be expressed in terms of the x component of the wavevector $k_{xP}(\theta)$ by $k_{zP}(\theta) = [(2\pi/\lambda)^2 \epsilon_P - k_{xP}^2(\theta)]^{1/2}$ with $k_{xP}(\theta) = (2\pi/\lambda) [\epsilon_P \sin^2 \theta]^{1/2}$, and ϵ_P is the dielectric constant of the prism. The detailed derivations of the SPR reflectance associated with MSEF are given elsewhere.^{4,5}

SPR of Nonabsorbing Dielectrics. For SPR of nonabsorbing dielectrics, absorption of the metal film is the only source for the reflection loss under the ATR condition. The SPR reflectance can then be expressed in terms of the absorption of the metal film by⁴

$$R(\theta) = 1 - \left(\frac{2\pi}{\lambda}\right)^2 \frac{1}{k_{zP}(\theta)} \int_0^{d_M} \text{Im}[\hat{\epsilon}_M] \langle E_z^2(\theta) \rangle dz \quad (2)$$

where d_M and $\hat{\epsilon}_M$, respectively, are the thickness and the complex dielectric constant of the metal film.

SPR–SPFS of Absorbing Dielectrics. The SPR curve of an absorbing dielectric is more complicated than that of the nonabsorbing dielectric due to the presence of an additional absorbing medium beside the metal film. When an absorbing dielectric is present in the sensor architecture, the evanescent field amplitude at the metal/dielectric interface becomes smaller.⁴ According to eq 1, the SPR reflectance with an absorbing dielectric film is given by

$$R(\theta) = 1 - \left(\frac{2\pi}{\lambda}\right)^2 \frac{1}{k_{zP}(\theta)} \left\{ \int_0^{d_M} \text{Im}[\hat{\epsilon}_M] \langle E_z^2(\theta) \rangle dz + \int_{d_{AD}} \text{Im}[\hat{\epsilon}_{AD}] \langle E_z^2(\theta) \rangle dz \right\} \quad (3)$$

where $\int_{d_{AD}}$ indicates an integration over the thickness of the absorbing dielectric film while d_{AD} and $\hat{\epsilon}_{AD}$, respectively, are thickness and complex dielectric constant of the absorbing dielectric film. Similar to that of the nonabsorbing dielectric, the resonance angle shifts linearly with the refractive index and/or thickness variation of the absorbing dielectric film.⁴ However, a broader SPR curve together with a greater reflectance minimum are observed as the dielectric film becomes highly absorbing.⁶

For binding events associated with a small number of molecules or molecules of small size (i.e., low surface coverage antibodies or short DNA fragments), an insig-

nificant resonance angle shift is observed. However, if the bound molecules contain fluorophores, SPFS is a powerful sensing technique for such binding phenomena. SPFS exhibits a strong fluorescence signal, while SPR shows insignificant change associated with the binding of small molecules.^{2,4} Although there is a linear relationship between the absorption and fluorescence of a fluorophore, the SPFS fluorescence signal is attenuated by fluorescence quenching via nonradiative RET to the metal film.^{3,7} Due to the distance-dependent nature of the RET phenomenon, the SPFS fluorescence signal shows distance-dependent characteristics. The fluorescence signal decreases substantially if fluorophores are confined closer to the metal film. Since RET phenomenon is not influenced by the angle of incidence, the SPFS fluorescence signal, $I_{\text{Fluorescence}}(\theta)$, from a sensor with a single layer of a fluorophore-containing dielectric film can be expressed in terms of the MSEF by⁴

$$I_{\text{Fluorescence}}(\theta) = K_{\text{Optics}} \left(\frac{2\pi}{\lambda}\right)^2 \frac{1}{k_{zP}(\theta)} \int_{d_{\text{Fluorophore}}} K_{\text{RET}}(z) \times \text{Im}[\hat{\epsilon}_{\text{Fluorophore}}] \langle E_z^2(\theta) \rangle dz \quad (4)$$

where $\hat{\epsilon}_{\text{Fluorophore}}$ is the dielectric constant of the film and $K_{\text{RET}}(z)$ is the fluorescence quenching factor. $\int_{d_{\text{Fluorophore}}}$ indicates an integration over the thickness of the layer with fluorophores. K_{Optics} is a constant whose value depends on experimental parameters (i.e., attenuation factor, filter, focusing lens, and optical windows).

Although parameters associated with the nonabsorbing dielectrics in the sensor architecture do not appear in the above equations, their influences manifest themselves in the observed SPR–SPFS signals. The resonance angle and the fluorescence angle (i.e., the angle with the maximum fluorescence signal) shift to a greater value as the thickness and/or refractive index of the nonabsorbing dielectric increase. The nonabsorbing dielectric film lying between the metal film and the fluorophore-containing dielectric film also serves as a spacer that decreases the fluorescence quenching. The greater is the separation of the fluorophores from the metal film, the smaller is the quenching efficiency.^{3b,4} The nonabsorbing dielectric spacer also alters the evanescent field amplitude within the absorbing dielectric. Due to its exponential decay characteristic, the evanescent field amplitude in the absorbing dielectric film decreases as its separation from the metal film increases. The greater separation results in a smaller amount of absorption and hence decreased fluorescence intensity.

Experimental Section

SPR–SPFS Setup. A schematic illustration of an SPR–SPFS setup is shown in Figure 1. For SPR measurement, a radiation from a HeNe laser ($\lambda = 632.8$ nm, 10 mW, Uniphase, San Jose, CA) is modulated by a chopper. The polarization and intensity of the modulated radiation are controlled by two Glan–Thompson polarizers (Owis, Germany). The radiation is coupled to the sensor via a right-angled prism (LASFN9, $\epsilon = 3.4036$, Schott Glas, Germany). The reflected beam is then focused ($f = 50$ mm, Owis, Germany) onto a photodiode detector. The corresponding SPFS fluorescence signal is simultaneously collected from the backside of the prism by focusing the emitted fluorescence through a set of filters (a neutral filter and an interference filter: $\lambda = 670$ nm, $\Delta\lambda = 10$ nm, LOT, 80% transmission) and onto a photomultiplier tube (Hamamatsu, Japan). The PMT is connected to a photon

(4) (a) Ekgasit, S.; Thammacharoen, C.; Knoll, W. *Anal. Chem.* **2004**, *76*, 561–568. (b) Ekgasit, S.; Thammacharoen, C.; Yu, F.; Knoll, W. *Anal. Chem.* **2004**, *76*, 2210–2219.

(5) Hansen, W. N. *J. Opt. Soc. Am.* **1968**, *58*, 380–390.

(6) (a) Baba, A.; Lübber, J.; Tamda, K.; Knoll, W. *Langmuir* **2003**, *19*, 9058–9064. (b) Baba, A.; Park, M. K.; Advincula, R. C.; Knoll, W. *Langmuir* **2002**, *18*, 4648–4652. (c) Lyon, L. A.; Peña D. J.; Natan, M. *J. J. Phys. Chem. B* **1999**, *103*, 5826–5831. (d) Wang, S.; Boussaad, S.; Tao, N. *J. Rev. Sci. Instrum.* **2001**, *72*, 3055–3060.

(7) (a) Valeur, B. *Molecular Fluorescence Principles and Applications*; Wiley-VCH: Weinheim, 2002. (b) Lakowicz, J. R. *Principles of Fluorescence Spectroscopy*, 2nd ed.; Kluwer Academic/Plenum Publishers: New York, 1999.

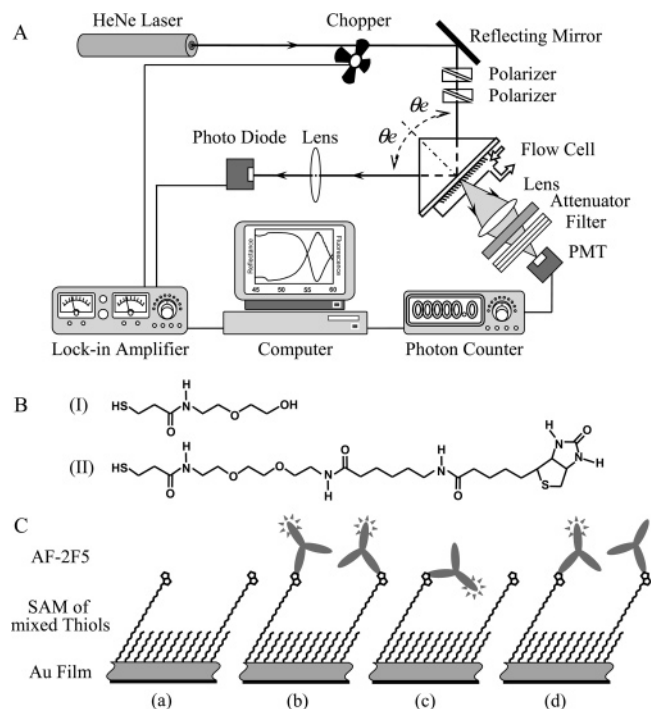


Figure 1. (A) A schematic illustration of the SPR–SPFS experimental setup. (B) The employed (I) OH-terminated thiol and (II) biotin-terminated thiol. (C) Schematic illustrations of the layer architectures associated with the binding events: (a) SAM of mixed thiols, (b) bound fluorophore-labeled AF-2F5 on the SAM surface, (c) the residual fluorophore-labeled AF-2F5 on the SAM surface after the regeneration, and (d) the residual fluorophore-labeled AF-2F5 after the binding of the nonlabeled 2F5. The illustrations are associated with the SPR and SPFS curves in Figures 2 and 3.

counter unit (Agilent, Palo Alto, CA) where the fluorescence signal is expressed in terms of photon counts per second (cps). The neutral filter, which is employed as an attenuator, keeps the signal from the PMP within its linear range (i.e., less than 1×10^6 cps). The current experiments employ an attenuation factor of 60.88. The factor is obtained from an independent calibration measurement.

The SPR–SPFS signals are collected as a function of the measured incidence angle, θ_e , defined with respect to the direction normal to the prism/metal interface. The measured incidence angle θ_e is slightly different from the incident angle θ at the prism/metal interface due to the refraction of the coupled radiation at the air/prism interface.⁴ For direct comparisons with the experimental results, the simulated results are expressed in terms of the measured incidence angle θ_e .

Biosensor Fabrication. LASFN9 glass wafers ($20 \times 20 \times 2.5$ mm³, Schott Glas, Germany) were cleaned and coated with an ~ 50 nm gold film via a commercially available thermal evaporation instrument (Edwards FL400, England) at deposition rate of 0.1 nm/s under UHV condition (5×10^{-6} mbar). Solutions of mixed thiols (OH-terminated thiol and biotin-terminated thiol with a net thiol concentration of 500 μ M at mole fractions of biotin-terminated thiol $\chi = 0.04, 0.02, 0.01,$ and 0.004) were prepared in absolute ethanol. The self-assembled monolayer (SAM) was fabricated by immersing the gold-coated LASFN9 wafers in the thiol solution overnight at room temperature. The wafers were rinsed thoroughly with absolute ethanol, blown-dry with dry nitrogen, and kept under argon until being used.

Materials. The antibiotin mouse monoclonal antibody 2F5 (isotype IgG_{1,k}) and the Alexa Fluor 647 monoclonal antibody labeling kit were purchased from Molecular Probes. The 2F5 antibody was labeled with Alexa Fluor 647 dye following a standard protocol provided by Molecular Probes. The dye-to-protein ratio was 4.4 as determined by UV–visible spectroscopy. For simplicity, the fluorophore-labeled antibody 2F5 is abbreviated as AF-2F5. Sodium dodecyl sulfate (SDS) and phosphate-buffered saline (PBS) tablets were purchased from Sigma-Aldrich.

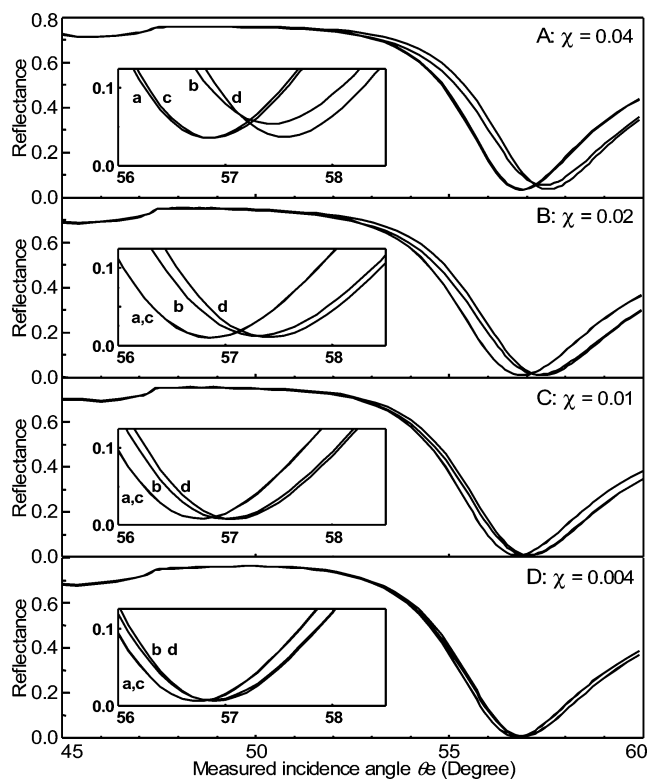


Figure 2. SPR curves of the systematic sensor fabrications at various mole fractions of biotin-terminated thiol: (A) $\chi = 0.04$, (B) $\chi = 0.02$, (C) $\chi = 0.01$, and (D) $\chi = 0.004$. The sensor architecture of each SPR curve is (a) Au/SAM, (b) Au/SAM/AF-2F5, (c) Au/SAM (regenerated), and (d) Au/SAM/2F5. The insets are added for clarity.

An HBS-EP buffer (degassed 10 mM HEPES-buffered saline, pH 7.4, 150 mM NaCl, 3 mM EDTA with 0.005% (v/v) surfactant P-20, Biacore, Sweden) was employed for the preparation of protein solutions.

All experiments were performed at room temperature (21 ± 2 °C) with HBS-EP as a buffer solution. A working concentration of 20 nM was employed for both labeled and nonlabeled antibodies. First, a 1 mL aliquot of fluorophore-labeled antibody AF-2F5 solution was injected into the flow cell. The solution is left in the flow cell for 15 min to allow a complete binding of the antibody onto the sensor surface. To remove bound antibodies, the sensor surface was flow-washed with SDS solution (5 mg/mL in HBS-EP). Once the regeneration is completed (i.e., no additional change in the observed SPR curve after prolonged washing), additional binding with nonlabeled antibody 2F5 was performed. Prior to all SPR–SPFS acquisitions, the cell was flow-washed and filled with running buffer to avoid bulk solution effect. Schematic illustrations of layer architectures of the biosensor associated with the binding and regeneration events are shown in Figure 1.

Results

The measured SPR curves of the systematic sensor fabrications are shown in Figure 2. The sensor architectures (i.e., complex dielectric constant and thickness) shown in Table 1 are obtained by fitting the observed SPR curves with Fresnel equation. The table indicates that there is sample-to-sample variation associated with the optical properties of the gold film. For SPR measurement, the resonance angle shifts to a greater value when the fluorophore-labeled AF-2F5 was bound onto the surface of the SAM. A greater magnitude of the resonance angle shift was observed at a greater mole fraction, χ . Small increments of reflectance minima were observed at high mole fractions ($\chi = 0.04$ and 0.02). However, the same phenomenon was not observed at lower mole fractions (χ

Table 1. Fitting Parameter of the Observed SPR Curves in Figure 2

SPR curve	layer architecture of biosensor ^a			experimental results ^c	
	complex dielectric constant ($\hat{\epsilon} = \epsilon' + i\epsilon''$)			θ_{SPR}	$\theta_{\text{Fluorescence}}$
	Au	SAM	AF-2F5 ^b or 2F5		
			A: $\chi = 0.04$		
a	-12.78 + <i>i</i> 1.42 51.00	2.25 1.40		56.9°	N/A
b	-12.78 + <i>i</i> 1.42 51.00	2.25 1.40	2.1025 + <i>i</i> 0.098 4.05	(AF-2F5) 57.4°	57.1°
c	-12.78 + <i>i</i> 1.42 51.00	2.25 1.40		56.9°	56.5°
d	-12.78 + <i>i</i> 1.42 51.00	2.25 1.40	2.1025 5.15	(2F5) 57.6°	57.2°
			B: $\chi = 0.02$		
a	-12.85 + <i>i</i> 1.58 46.90	2.25 1.30		56.8°	N/A
b	-12.85 + <i>i</i> 1.58 46.90	2.25 1.30	2.1025 + <i>i</i> 0.037 3.30	(AF-2F5) 57.3°	56.7°
c	-12.85 + <i>i</i> 1.58 46.90	2.25 1.30		56.8°	56.4°
d	-12.85 + <i>i</i> 1.58 46.90	2.25 1.30	2.1025 4.10	(2F5) 57.4°	56.9°
			C: $\chi = 0.01$		
a	-12.94 + <i>i</i> 1.54 46.90	2.25 1.20		56.8°	N/A
b	-12.94 + <i>i</i> 1.54 46.90	2.25 1.20	2.1025 + <i>i</i> 0.010 1.80	(AF-2F5) 57.0°	56.5°
c	-12.94 + <i>i</i> 1.54 46.90	2.25 1.20		56.8°	56.3°
d	-12.94 + <i>i</i> 1.54 46.90	2.25 1.20	2.1025 2.30	(2F5) 57.1°	56.6°
			D: $\chi = 0.004$		
a	-12.94 + <i>i</i> 1.48 47.10	2.25 1.10		56.8°	N/A
b	-12.94 + <i>i</i> 1.48 47.10	2.25 1.10	2.1025 + <i>i</i> 0.006 1.00	(AF-2F5) 56.9°	56.5°
c	-12.94 + <i>i</i> 1.48 47.10	2.25 1.10		56.8°	56.4°
d	-12.94 + <i>i</i> 1.48 47.10	2.25 1.10	2.1025 1.10	(2F5) 56.9°	56.5°

^a An LASFN9 Glass ($\hat{\epsilon} = 3.4036$) is employed as a coupling prism, while the HBS-EP buffer ($\hat{\epsilon} = 1.778$) is employed as a semi-infinitely thick nonabsorbing dielectric substrate. ^b AF-2F5 is the fluorophore-labeled antibody. ^c The measure angle of incidence, θ_e , has a resolution of 0.1° near the resonance angle.

= 0.01 and 0.004), i.e., the reflectance minimum remains unchanged after the binding of the antibody. When the sensor was regenerated, the observed SPR curve superimposed with that of the virgin SAM. However, an imperfect superimposition is observed at $\chi = 0.04$. When the nonlabeled 2F5 was bound onto the regenerated surface, the resonance angle shifts to a greater value. The magnitude of the angle shift is slightly larger than that of the corresponding fluorophore-labeled antibody. This phenomenon indicates a preferred binding of biotin toward the nonlabeled antibody. In agreement with the theoretical prediction, a change in the magnitude of the minimum reflectance was not observed after the binding of the nonlabeled antibody.

The corresponding SPFS curves are shown in Figure 3. When the fluorophore-labeled AF-2F5 was bound onto the nonfluorescing SAM, a strong fluorescence signal was observed. The fluorescence signal increases as the mole fraction, χ , increases. Although the fluorescence angle shifts in the same fashion as the resonance angle, the fluorescence angle is slightly smaller than the corresponding resonance angle (see Table 1). After the regeneration process, the fluorescence signal decreases substantially as the fluorophore-labeled antibody was removed. Although the corresponding SPR curve of the regenerated sensor is superimposed with that of the virgin sensor (except that with $\chi = 0.04$), a significant fluorescence signal of the regenerated sensor could still be observed. A stronger fluorescence signal is observed from

the sensor with a greater mole fraction, χ . Interestingly, the fluorescence signal increases as the nonlabeled antibody was additionally bound onto the regenerated sensor. A greater fluorescence increment was observed in the sensor with a greater mole fraction, χ .

Discussion

As shown in Table 1, effective thickness of the SAM increases as the mole fraction, χ , of the long-chain biotin-terminated thiol increases. The thicker SAM indicates a greater number of available biotin binding site on the sensor surface. The larger number of biotin binding site is experimentally confirmed by a greater magnitude of the resonance angle shift after the binding events. When the thickness of the dielectric film is increased by the binding phenomena, the resonance angle shifts to a greater value. Since the magnitude of the shift has a linear relationship with the thickness of the dielectric film, a SAM with a greater mole fraction, χ , induces a greater shift. The unchanged reflectance minimum after the binding of the nonlabeled antibody is due to the unchanged evanescent field maximum at the metal/dielectric interface as it shifts to a greater value by a greater nonabsorbing dielectric film thickness. The presence of a weakly absorbing dielectric, on the other hand, slightly decreases the field amplitude at the interface. As a result, after the binding of the fluorophore-labeled antibody, slightly greater reflectance minimums are observed at $\chi = 0.04$ and 0.02. At lower mole fractions, $\chi = 0.01$ and 0.004, the

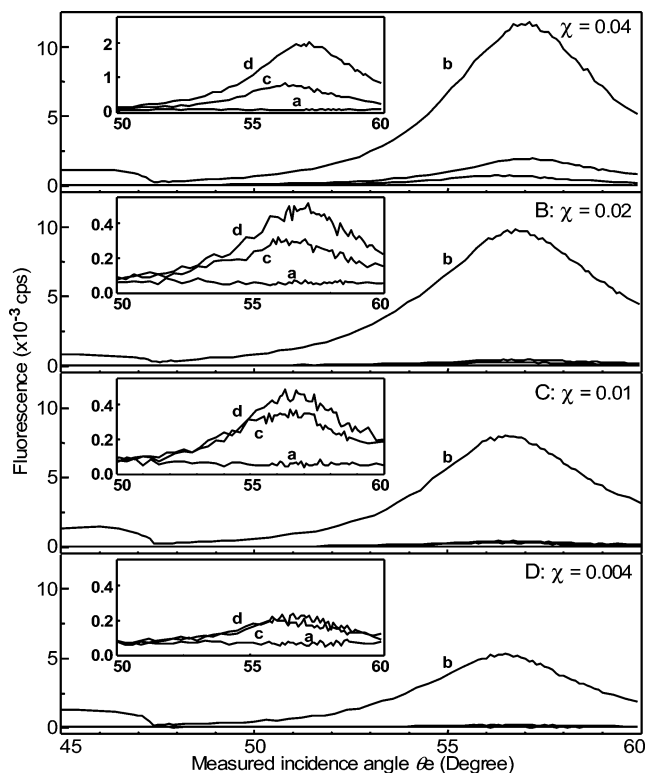


Figure 3. The corresponding SPFS curves of the systems shown in Figure 2: (A) $\chi = 0.04$, (B) $\chi = 0.02$, (C) $\chi = 0.01$, (D) $\chi = 0.004$. The insets are added for clarity.

unchanged reflectance minimums are due to weak absorptions. However, evidence of the weak absorptions is clearly seen in the strong fluorescence signal of the corresponding SPFS curves. This observation demonstrates the capability of the SPFS technique for obtaining information about the chemical nature of the fluorescing dielectric film. By relying on the SPR signal alone, such a film might otherwise be mistaken as a nonabsorbing dielectric.

The slightly smaller fluorescence angle compared to the resonance angle arises from two factors: the angle-dependent nature of the wavevector and the decay characteristics of the evanescent field.⁴ The evanescent field at the metal/dielectric interface on the dielectric side has the maximum at a slightly smaller angle than that on the metal side. The evanescent field in the dielectric film decays with the field maximum tailing toward a smaller angle while that in the metal film tails toward a greater angle. As a result, SPR reflectance, which is dominated by the absorption of metal film, has a minimum at an angle slightly greater than the fluorescence angle of the corresponding SPFS fluorescence, which is governed by the absorption of the dielectric.⁴ Although the fluorescence intensity is directly correlated to the absorption of the fluorophores, the concentration of the absorbing species on the sensor surface (i.e., number of the labeled antibody per unit area) cannot be directly derived from the observed SPFS fluorescence signal. This is due to the distance-dependent fluorescence quenching, the sample-to-sample variation associated with the optical constant of the metal film, and the thickness of the dielectric film associated with the employed dielectric constant.⁸

As the sensor is regenerated, the superposition between the regenerated SAM and the virgin SAM indicates

stability of the biotin-functionalized surface. The imperfect superposition of the SPR curve at $\chi = 0.04$ is due to the greater number of residual fluorophore-labeled antibody associated with a greater number of biotin binding sites. The strong fluorescence signal of the regenerated sensor suggests a residual fluorophore-labeled antibody on the biosensor surface. However, the absorption of the residual fluorophore-labeled antibody is too small to induce a significant shift in the reflectance minimum. This phenomenon confirms the superiorly sensitive nature of SPFS associated with extremely small numbers of bound fluorophore-labeled molecules.

The increments of fluorescence signals after the binding of the nonlabeled antibody signify the displacement of the residual fluorophore-labeled antibody from the SAM surface. Due to the flexibility of long-chain biotin-terminated thiols and the extremely low surface coverage of the residual fluorophore-labeled antibody after the regeneration, the antibody lies close to the SAM surface. When an additional nonlabeled antibody was bound onto the abundantly available biotin binding sites, the residual fluorophore-labeled antibody is forced to displace away from the SAM surface due to the constraint imposed by the nonlabeled antibody. The weaker fluorescence quenching due to a greater separation of fluorophore from the gold surface results in the increment of the observed fluorescence signal. Although a quantitative analysis of the fluorescence signal is not possible due to the unknown fluorescence quenching efficiency, information about the displacement of the residual fluorophore-labeled antibody can be obtained via analysis of the evanescent field decay profile within the dielectric medium since the comparison is made within the same sensor. Although the exact distances of the fluorophore from the gold film before and after the binding cannot be calculated, their relative distances from the gold film can be compared. The system with $\chi = 0.02$ is chosen as an example. Due to the extremely low concentration of fluorophore-labeled antibody, no resonance energy transfer via self-quenching by neighboring dye molecules is assumed.⁹ If the layer of the residual fluorophore-labeled antibody on the regenerated SAM was to arrange in such a way that it experiences the same quenching efficiency as that after the binding of the nonlabeled antibody, it must have the equal thickness of 4.10 nm (see Table 1). It should be noted that this layer is an imaginary layer since the optical parameters in Table 1 indicate that the thickness of the residual fluorophore-labeled antibody layer equals zero (i.e., its SPR curve superimposes with that of virgin SAM). Due to the extremely low surface coverage of the residual fluorophore-labeled antibody, the dielectric constant of the layer is assumed to be the same as that of the buffer ($\epsilon = 1.778$). If there is no desorption of the residual fluorophore-labeled antibody during the binding of the nonlabeled antibody, the imaginary part of the dielectric constant of the layer stays unchanged since the layer is extremely weak absorbing while the volume of the layer stays unchanged. According to eqs 3 and 4, the fluorescence intensity is linearly proportional to the integration of the evanescent field within the absorbing layer. Figure 4 shows superposition of the observed SPFS curves and the corresponding evanescent field integration within the layer with the residual fluorophore-labeled antibody. An excellent agreement between observation and theoretical prediction is observed (SPFS curve shape and the fluorescence angle). The evanescent field amplitude at the metal/dielectric

(8) Peterlinz, K. A.; Georgiadis, R. *Opt. Commun.* **1996**, *130*, 260–266.

(9) (a) Buschmann, V.; Weston, K. D.; Sauer, M. *Bioconjugate Chem.* **2003**, *14*, 195–204. (b) Anderson, G. P.; Nerurkar, N. L. *J. Immunol. Methods* **2002**, *271*, 17–24.

Table 2. Comparison between Observed the SPFS Fluorescence Signal in Figure 3 and the Evanescent Field Integration at the Resonance Angle before and after Additional Binding of the Nonlabeled Fluorophore

SPFS curve	fluorescence signal ($\times 10^{-3}$ cps) ^a		$(2\pi/\lambda)^2 1/k_{zP} \int \langle E_z^2 \rangle dz$ (arbitrary unit)	
	after regeneration (SPFS curve c)	after 2F5 binding (SPFS curve d)	after regeneration ^b	after 2F5 binding ^c
$\chi = 0.04$	0.69	1.91	1.80	1.36
$\chi = 0.02$	0.24	0.44	1.37	1.03
$\chi = 0.01$	0.26	0.41	0.80	0.60
$\chi = 0.004$	0.14	0.17	0.40	0.30

^a Fluorescence signal with baseline correction. ^b Calculated on the basis of optical parameters in Table 1 (SPR Curve c) with the thickness of the residual fluorophore-labeled antibody of 4.10 nm and $\epsilon = 1.778$. ^c Calculated On the basis of optical parameters in Table 1 (SPR Curve d).

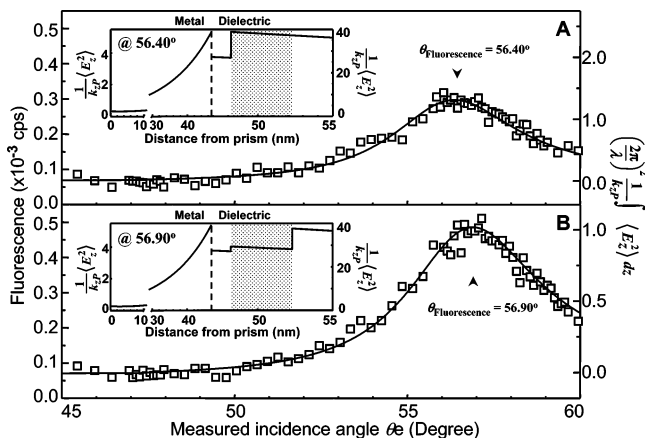


Figure 4. The superposition of the observed SPFS curve and the corresponding evanescent field integration within the fluorophore-containing layers at a mole fraction of biotin-terminated thiol $\chi = 0.02$ (A) after the regeneration and (B) after the binding of nonlabeled antibody. The insets show the evanescent field decay profile at the fluorescence angles. The optical parameters in Table 1 are employed for the calculation. The layer of residual fluorophore-labeled antibody in (A) is assumed to have the same thickness as that in (B) with a dielectric constant of $\epsilon = 1.778$. Note: the scales on the field integration axes of both figures are not the same.

interface becomes greater as the refractive index of the dielectric film becomes smaller.⁴ A greater evanescent field integration in Figure 4A compared to that in Figure 4B suggests that a stronger fluorescence signal would have been observed before the binding of the nonlabeled antibody if the residual fluorophore-labeled antibody were to arrange by the assumed fashion (i.e., with a thickness of 4.10 nm). However, opposite phenomena were experimentally observed at every mole fraction, χ (see Table 2). The only explanation of this contradiction is that the residual fluorophore-labeled antibody lies closer to the SAM surface before the binding of the nonlabeled antibody. Thus, the fluorophore experiences strong fluorescence quenching. The greater fluorescence signal after the binding is due to the displacement of the fluorophore-labeled antibody away from the SAM surface where the fluorescence quenching is smaller. The greater number of neighboring molecules at the higher mole fraction, χ , imposes a greater displacement.

It should be noted that the sensitivity of the current experiment could be increased up to 60 times by decreasing the attenuation factor of the neutral filter. Additional improvements can be achieved by modifying the optical setup and/or using thiol with a longer chain length. For a different fluorescing dye, an appropriate excitation wavelength can be employed.

Conclusions

The highly sensitive nature of fluorescence spectroscopy combined with a strong surface-plasmon-wave-generated

evanescent field enables SPFS to detect binding events associated with extremely small numbers of fluorophore-labeled molecules, which cannot be observed by the SPR technique alone due to an insufficient thickness change. Although the nonradiative RET near the metal surface quenches the fluorescence from the excited fluorophore, its distance-dependent nature can be employed to monitor the relative distance of the fluorophore-containing antibody from the metal film. The displacement of a fluorophore-containing antibody due to the steric constraints imposed by neighboring nonlabeled antibodies is proportional to the number of available binding sites. The displacement was theoretically explained via the relationship between the SPFS fluorescence intensity and the surface-plasmon-wave-generated evanescent field. The observed phenomena indicate that SPR-SPFS can be employed for determining and/or monitoring movement of molecules near the metal surface.

Appendix

The complex dielectric constant of a mixture can be expressed in terms of those of the mixed components by

$$\hat{\epsilon}_{mix} = \epsilon'_{mix} + i\epsilon''_{mix} = \sum_{i=1}^m \phi_i \hat{\epsilon}_i = \sum_{i=1}^m \phi_i (\epsilon'_i + i\epsilon''_i) = \sum_{i=1}^m \phi_i (n_i + ik_i)^2 = \sum_{i=1}^m \phi_i [(n_i^2 - k_i^2) + i2n_i k_i]$$

where m is the number of the mixed components, ϕ_i , $\hat{\epsilon}_i$, n_i , and k_i , respectively, are the volume fraction, the complex dielectric constant, the refractive index, and the absorption index of the i^{th} component. When an absorbing dielectric is dissolved by two different nonabsorbing dielectrics, if the volume fraction of the absorbing dielectric is kept constant, the imaginary parts of the dielectric constant of both solutions are the same, see the above equation. According to eq 1, the absorption under the ATR condition is proportional to the imaginary part of the dielectric constant ϵ'' . However, their absorptions are not equal due to the dependence of the evanescent field amplitude on the refractive index (or the real part of the dielectric constant).

Acknowledgment. S.E. gratefully acknowledges support from the National Research Council of Thailand (NRCT) under the Nanopolymer Project (Kor-Sor-Sor 52/2547) and the Alexander von Humboldt (AvH) Foundation.